Progress in Oceanography 186 (2020) 102393

Contents lists available at ScienceDirect

Progress in Oceanography

journal homepage: www.elsevier.com/locate/pocean

Evaluating ecosystem change as Gulf of Alaska temperature exceeds the limits of preindustrial variability

Michael A. Litzow[a,*], Mary E. Hunsicker[b], Eric J. Ward[c], Sean C. Anderson[d], Jin Gao[c,e], Stephani G. Zador[f], Sonia Batten[g], Sherri C. Dressel[h], Janet Duffy-Anderson[f], Emily Fergusson[i], Russell R. Hopcroft[j], Benjamin J. Laurel[k], Robert O'Malley[l]

[a] College of Fisheries and Ocean Sciences, University of Alaska Fairbanks, Kodiak, AK 99615, USA
[b] Northwest Fisheries Science Center, National Marine Fisheries Service, Newport, OR 97365, USA
[c] Northwest Fisheries Science Center, National Marine Fisheries Service, Seattle, WA 98112, USA
[d] Pacific Biological Station, Fisheries and Oceans Canada, Nanaimo, BC V9T 6N7, Canada
[e] Centre for Fisheries Ecosystems Research, Memorial University of Newfoundland, St. John's, NL A1C 5R3, Canada
[f] Alaska Fisheries Science Center, National Marine Fisheries Service, Seattle, WA 98115, USA
[g] Marine Biological Association, Nanaimo, BC V9V 1N8, Canada
[h] Division of Commercial Fisheries, Alaska Department of Fish and Game, Juneau, AK 99811, USA
[i] Alaska Fisheries Science Center, National Marine Fisheries Service, Juneau, AK 99801, USA
[j] College of Fisheries and Ocean Sciences, University of Alaska Fairbanks, Fairbanks, AK 99775, USA
[k] Alaska Fisheries Science Center, National Marine Fisheries Service, Newport, OR 97365, USA
[l] Department of Botany and Plant Pathology, Oregon State University, Corvallis, OR, 97331, USA

ARTICLE INFO

Keywords:
Bayesian Dynamic Factor Analysis
Climate change
Climate variability
Gulf of Alaska
Ecosystem response
Nonstationary relationship

ABSTRACT

The Gulf of Alaska experienced extreme temperatures during 2014–2019, including the four warmest years ever observed. The goal of this study is to evaluate the ecological consequences of that warming event, across multiple trophic levels and taxa. We tested for evidence that observed sea surface temperature (SST) anomalies were outside the envelope of natural climate variability in order to evaluate the risk of novel ecosystem configurations. We also tested for state changes in shared trends of climate (n = 11) and biology (n = 48) time series, using a Bayesian implementation of Dynamic Factor Analysis (DFA). And we tested for evidence of novel ecological relationships during 2014–2019. We found that 3-year running mean SST anomalies during 2014–2019 were outside the range of anomalies from preindustrial simulations in CMIP5 models, indicating that the combined magnitude and duration of the warming event was outside the range of natural variability. A DFA model of climate variability also returned a shared trend in climate time series that was at unprecedented levels during 2014–2019. However, DFA models fit to biology data did not show shared trends of variability at unprecedented levels, and Hidden Markov Models fit to shared trends from the climate and biology models failed to find evidence of shifts to a new ecosystem state during 2014–2019. Conversely, we did find preliminary indications that community responses to SST variability strengthened during 2014–2019 after decades of a mostly neutral relationship. Tests for nonstationary patterns of shared variability suggest that covariance between SST and other ecologically-important climate variables remained weaker than during the 1970s Pacific Decadal Oscillation shift, suggesting the potential for muted ecological responses to the 2014–2019 event. Finally, we found that recent patterns of community variability appear to be highly dissimilar to those associated with the 1970s event, suggesting the potential for novel community states with continued warming. In summary, we find no evidence for wholesale ecosystem reorganization during 2014–2019, though nonstationary relationships among climate and community variables suggest the ongoing possibility of novel patterns of ecosystem functioning with continued warming.

* Corresponding author at: Alaska Fisheries Science Center, National Marine Fisheries Service, 301 Research Ct., Kodiak, AK 99615, USA.
E-mail address: mike.litzow@noaa.gov (M.A. Litzow).

https://doi.org/10.1016/j.pocean.2020.102393
Received 12 February 2020; Received in revised form 10 June 2020; Accepted 17 June 2020
Available online 22 June 2020
0079-6611/ Published by Elsevier Ltd.

1. Introduction

The North Pacific Ocean was unprecedentedly warm for much of 2014–2019. This climate event at first appeared to be part of a discrete multi-year heatwave characterized by extremely high sea level pressure (SLP) anomalies that led to reduced wind mixing and wind-forced advection, resulting in extreme ocean temperatures (the "Warm Blob"; Bond et al., 2015). Attribution studies suggest that peak temperatures during this event, in 2016, would have been impossible absent anthropogenic radiative forcing (Jacox et al., 2018; Walsh et al., 2018b). After more normal temperatures in 2017, extreme temperatures returned in 2018–2019, establishing the climate perturbation as a longer time scale event rather than a discrete heatwave.

The North Pacific provides a range of important ecosystem services, including commercial and subsistence fisheries that are critical for the cultural, social, and economic well-being of coastal communities. Understanding the ecosystem implications of the 2014–2019 warm anomaly is important both for appropriate management of these ecosystem services under accelerating physical stress, and to inform societal decisions concerning the mitigation of, and adaptation to, global warming and other aspects of human-caused climate change. A number of biological responses to the climate perturbation have already been noted in the northern North Pacific (Bering Sea and Gulf of Alaska). These include the largest-ever observed mass mortality event for common murres (Piatt et al., 2020) and a variety of other seabird mass mortality events; acute and chronic production of neurotoxins by harmful algal blooms (McCabe et al., 2016; Roggatz et al., 2019); unusual mortality for humpback whales (*Megaptera novaeangliae*) in the western Gulf of Alaska in 2015[1]; unprecedented irruptions of pelagic colonial tunicates (*Pyrosoma* sp.) in the Gulf of Alaska in 2017[2,3]; fisheries failures for Gulf of Alaska Pacific cod (*Gadus marocephalus)* in 2018[4], Gulf of Alaska-wide pink salmon (*Onchorynchus gorbuscha*) runs in 2016[4], and Chignik Management Area sockeye salmon (*O. nerka*) in 2018[4]; dramatic abundance increases for Pacific cod and walleye pollock (*Gadus chalcogrammus*), and abundance decreases for Arctic cod (*Boreogadus saida*) in the northern Bering Sea (Stevenson and Lauth, 2019); drastic reductions in the energy content of Pacific sandlance (*Ammodytes personatus*), a key forage species (von Biela et al., 2019); and a delayed spring bloom and depressed abundance of large crustacean zooplankton in the southeast Bering Sea (Duffy-Anderson et al., 2019). However, understanding of the community-level impacts of this event remains limited. Summaries of effects across multiple taxonomic groups and trophic levels tend to be qualitative collections of multiple observations (e.g.; Cavole et al., 2016; Leising et al., 2015; Morgan et al., 2019), while more quantitative syntheses tend to concentrate on restricted trophic or taxonomic groups (e.g.; Auth et al., 2018; Brodeur et al., 2019; Gomez-Ocampo et al., 2018; Peterson et al., 2017). These studies have provided important summaries of ecosystem impacts of the warming event. We build on this foundation with a quantitative synthesis of impacts across all available long-term biology time series, for multiple trophic and taxonomic groups, in the Gulf of Alaska ecosystem.

Climate change complicates the task of evaluating ecosystem responses to physical forcing. There is a long history of studies testing for state shifts in ecosystem properties in the North Pacific, typically related to red noise in leading modes of internal climate variability (e.g., Hare and Mantua, 2000; Litzow and Mueter, 2014; Mantua et al., 1997). Testing for similar changes in mean values of ecosystem properties remains an important aspect of evaluating the impact of the 2014–2019 warming event. However, climate change also involves change to a suite of environmental variables beyond temperature. Because rates of change differ among different variables, novel combinations of physical variables are likely to occur as anthropogenic change accelerates (Henson et al., 2017; Wolkovich et al., 2014). These new combinations are indicated by correlations among climate variables that are nonstationary, or described by probability distributions that change over time (Kolmogorov, 1991). Novel climate combinations expose communities to new combinations of physical forcing variables, with the potential result of reorganized biological communities that are poorly described by existing ecological understanding (Maguire et al., 2015; Williams and Jackson, 2007).

In the Gulf of Alaska, both types of ecosystem change (shifts in mean ecosystem state and nonstationary relationships among ecologically-important climate variables) are intimately related to dynamics in the Aleutian Low, an area of climatological low atmospheric surface pressure during the winter in the northern North Pacific (Trenberth and Hurrell, 1994). At a basin scale, the Aleutian Low drives wind stress fields that regulate water column mixing, Ekman transport, and heat fluxes that contribute to the Pacific Decadal Oscillation (PDO) sea surface temperature (SST) pattern (Newman et al., 2016). At a regional scale, the Aleutian Low drives cyclonic mean atmosphere and ocean circulation in the Gulf of Alaska, which in turn affects regional-scale physical variables including temperature, wind stress, advection, coastal downwelling, coastal freshwater discharge, coastal salinity, and nutrient availability (Coyle et al., 2019; Hunt et al., 2008; Weingartner et al., 2005). During the 20th Century, low-frequency change in the average intensity of the Aleutian Low was a primary driver of shifts between persistently positive and negative values in the PDO index (Mantua et al., 1997). During that time, community composition for Gulf of Alaska fish and crustaceans tracked the PDO index in a linear fashion (Hare and Mantua, 2000; Litzow and Urban, 2009). Broadly speaking, negative PDO values were associated with a community state rich in crabs, shrimp, and lipid-rich forage fishes, while positive PDO values were associated with increased abundance of salmon (*Oncorhynchus* spp.) and groundfishes such as Pacific cod and Pacific halibut (*Hippoglossus stenolepis*; Anderson and Piatt, 1999; Hare and Mantua, 2000; Litzow et al., 2014). In the late 1980 s, though, the Aleutian Low experienced a sharp decline in interannual variance (Litzow et al., 2020, 2018). Strong departures from average atmospheric forcing conditions (strong positive or negative anomalies in SLP) were no longer present. Absent strong contrasts in atmospheric forcing, previously strong correlations between Aleutian Low SLP values and regional climate variables in the Gulf of Alaska degraded towards zero. Strong intercorrelation among regional climate variables that had previously reacted synchronously to Aleutian Low variability also decayed, and in particular, previously strong relationships between regional SST and other important climate variables, as well as strong relationships between the PDO index and regional climate variables, degraded. Apparently as a result, previously strong correlations between SST/PDO variability and community state largely disappeared (Litzow et al., 2020, 2019, 2018; Puerta et al., 2019).

The goal of the current study is to evaluate the evidence for either state changes (shifts in mean state across multiple climate and biology time series) or nonstationary ecological relationships (changing correlations among variables) in the Gulf of Alaska ecosystem during the 2014–2019 climate anomaly. Departure from the natural range of climate variability implies an increased chance of novel system configurations and ecological surprises (Williams and Jackson, 2007). We therefore also test the hypothesis that the magnitude and duration of 2014–2019 temperature anomalies were outside the envelope of natural variability, in order to evaluate the degree to which this event may represent a transition to a novel anthropogenic climate state. Our

[1] https://www.fisheries.noaa.gov/national/marine-life-distress/2015–2016-large-whale-unusual-mortality-event-western-gulf-alaska

[2] https://www.fisheries.noaa.gov/resource/data/2017-status-alaska-marine-ecosystems-considerations-gulf-alaska

[3] https://www.fisheries.noaa.gov/feature-story/researchers-investigate-explosion-number-pyrosomes-alaska

[4] https://www.fisheries.noaa.gov/national/funding-and-financial-services/fishery-disaster-determinations

specific objectives are to: 1) calculate the fraction of risk for SST anomalies throughout the 2014–2019 period that can be attributed to anthropogenic forcing; 2) evaluate the evidence for state changes in shared trends of multivariate climatic and biological variability; 3) test for nonstationary community responses to SST variability since 2014; and 4) test for nonstationary associations among individual climate and biology time series. An important contribution of this study is the development and application of a Bayesian implementation of Dynamic Factor Analysis (DFA) to provide probabilistic statements about how time series map onto shared unseen processes (Ward et al., 2019).

2. Methods

2.1. Comparing SST observations to preindustrial simulations

For objective 1, we evaluated the evidence that 2014–2019 SST anomalies exceeded the limits of preindustrial variability by calculating the Fraction of Attributable Risk (FAR; 1 - $Prob_{preindustrial}$ / $Prob_{present}$) (Stott et al., 2004; Walsh et al., 2018b). We calculated FAR both for SST anomalies in each year, and for non-overlapping three-year running mean anomalies in order to compare the combined duration and magnitude of recent climate conditions with those expected under preindustrial conditions (Jacox et al., 2018). FAR values were calculated with previously-published outputs from five climate models run under preindustrial conditions as part of the Coupled Model Intercomparison Project Phase 5 (CMIP5). These five models were judged to be the best CMIP5 models for capturing Arctic variability (Walsh et al., 2018b, 2018a). Model SST outputs were summarized for the area 50°-60°N, 150°-130°W. Observed SST for the same area was calculated as the area-weighted mean of monthly ERSSTv5 values (Huang et al., 2017), and converted to anomalies by subtracting the 1981–2010 mean and dividing by the 1900–2016 standard deviation (following the approach used by Walsh et al. [2018b]). Valid comparisons of three-year running means between observations and simulations requires that models capture the autocorrelation (red noise) that is a natural feature of SST due to the thermal inertia of water (Di Lorenzo and Ohman, 2013; Newman et al., 2016). First-order autocorrelation during 1987–2005 (the period of historical simulations used by Walsh et al. [2018b]) was broadly similar for observations (0.29) and four of the five models (range 0.27 – 0.49). A fifth model (MRI.CGCM3) showed markedly lower autocorrelation (-0.04) and was therefore dropped from the three-year running mean comparison. For the calculation of FAR values, the probability of observed anomalies under preindustrial values was estimated from single 60-year windows randomly selected for each model (Walsh et al., 2018b), and the probability under the current climate was calculated for the 1960–2019 reference period (matching the 60-year length of preindustrial simulations). We also compared the magnitude of change associated with the 2014–2019 anomaly (in normalized units) with the magnitude of change around the 1976/77 PDO shift, as an approach for evaluating the size of the 2014–2019 perturbation relative to a historical event with profound and long-lasting ecological consequences.

2.2. Climate and biology data

We used a wide range of climate and biology time series to characterize Gulf of Alaska ecosystem variability (Table 1). For climate data, we used our familiarity with the study system to select a parsimonious set of variables (n = 11) to capture ecologically-important physical properties (Fig. 1). These included winter (November-March) and spring (May-June) SST for both the western and eastern Gulf of Alaska, the SLP gradient between Ketchikan and Seward (a proxy for onshore windflow and resulting orographic precipitation / freshwater input; Weingartner et al., 2005), February-April 20 m salinity at the GAK1 site, the Ocean Station Papa index (a measure of gyre-scale advection), and Bakun upwelling indices for four stations (54°N 134°W, 57°N 137°W, 60°N 146°W, 60° 149°W) during summer (May-July), the season when persistent coastal downwelling in this system relaxes (Stabeno et al., 2004).

We populated the biology data sets for this study by searching for all available time series that met the following criteria. We wanted to detect community responses to climate change without long lags, so we used population parameters that are expected to show short (0- or 1-year lag) responses to climate variability. Because we wanted to compare recent biological variability to longer-term patterns, we only used time series that were at least 15 years long. The resulting list of time series (n = 48) included: abundance and phenology estimates for short-lived taxa (phytoplankton, zooplankton, forage fish, jellyfish, shrimp) or early life history stages of long-lived taxa (ichthyoplankton); the nearshore abundance of one groundfish with a history of rapid changes in abundance and distribution in response to climate variability (Pacific cod); a growth chronology for another groundfish (northern rockfish *Sebastes polyspinis*); and commercial catches of pink salmon and coho salmon (*Oncorhynchus kisutch*), species which return to natal rivers one year after ocean entry, and thus show short-lag abundance responses to ocean conditions.

Biology data were normalized with log transformations, or fourth-root transformations for time series containing zeros, as needed. For example, if the time series data were lognormal (e.g. weight/count data) or the coefficient of variation was > 1, the data were normalized. Ichthyoplankton data were standardized using Generalized Additive Models prior to analysis to account for spatial and temporal variability in sampling effort among years (Marshall et al., 2019).

2.3. Testing for state changes

We describe these methods in detail below, but in summary, our work flow for objectives 2–4 was to (1) identify shared trends in multivariate climate and biology datasets; (2) evaluate the evidence for shifts in those shared ecosystem trends since 2014; (3) where time series length allowed, apply time-varying regressions to evaluate changing relationships between biological indices and SST since 2014; and (4) evaluate the evidence for changing relationships among individual time series within climate and biology data sets.

To summarize shared trends of climatic and biological variability, we implemented a Bayesian version of Dynamic Factor Analysis (DFA, Zuur et al., 2003b, Ward et al. 2019) using the software Stan and R (Carpenter et al., 2017; R Core Team, 2018; Stan Development Team, 2018). DFA is a multivariate statistical tool somewhat analogous to Principal Components Analysis, but for time series data (Holmes et al., 2018; Zuur et al., 2003b). For a collection of time series, the number of unobserved, "latent" trends is specified *a priori*, and DFA estimates these latent trends as independent random walks. In mathematical form, this is expressed as

$$x_{t,i} = x_{t-1,i} + \varepsilon_{t-1,i},$$

where $x_{t,i}$ represents the value of latent (unobserved) trend i at time t, and the process error deviations $\varepsilon_{t-1,i}$ are generally assumed to have arisen from a multivariate distribution (with an identity covariance matrix for identifiability; Zuur et al., 2003a). The latent trends at time t ($\mathbf{x}_t$) are mapped to the observed data $\mathbf{y}_t$ through a loadings matrix $\mathbf{Z}$ and residual error δ_t,

$$\mathbf{y}_t = \mathbf{Z}\mathbf{x}_t + \delta_t.$$

Because the response is multivariate, $\mathbf{y}_t$ represents the value of all time series at time t. The residual error terms are assumed to be drawn from a univariate or multivariate normal distribution, where variances may be shared or not across time series, as well as correlated or not.

Our Bayesian implementation of DFA provides a probabilistic summary of multivariate time series relationships. We present posterior distributions that allow the plausible range of time series loadings and shared trends to be evaluated. Our implementation is more flexible than

Table 1
Data and sources for evaluating multivariate climate and biology variability.

Variable	Metric	Years	Source
Climate			
Sea surface temperature anomaly, °C	Western Gulf of Alaska, Nov-Mar	1950–2019	ERSSTv5
Sea surface temperature anomaly, °C	Western Gulf of Alaska, Apr-Jun	1950–2019	ERSSTv5
Sea surface temperature anomaly, °C	Eastern Gulf of Alaska, Nov-Mar	1950–2019	ERSSTv5
Sea surface temperature anomaly, °C	Eastern Gulf of Alaska, Apr-Jun	1950–2019	ERSSTv5
Gyre scale advection	Papa advection index	1950–2019	NOAA Alaska Fisheries Science Center
Sea level pressure gradient (hPa)	SLP difference between Ketchikan and Seward (annual mean)	1950–2019	NCEP NCAR reanalysis
30 m salinity (PSU)	GAK1 Feb-Apr mean	1971–2017	University of Alaska
Downwelling, $m^3\ s^{-1}\ 100\ m^{-1}$ coastline	Jun-Aug mean at 60°N, 149°W	1950–2019	NOAA Pacific Marine Environmental Laboratory
Downwelling, $m^3\ s^{-1}\ 100\ m^{-1}$ coastline	Jun-Aug mean at 60°N, 146°W	1950–2019	NOAA Pacific Marine Environmental Laboratory
Downwelling, $m^3\ s^{-1}\ 100\ m^{-1}$ coastline	Jun-Aug mean at 57°N, 137°W	1950–2019	NOAA Pacific Marine Environmental Laboratory
Long-term biology			
Northern shrimp (*Pandalus eous*)	Pavlof Bay catch per unit effort, log-transformed	1972–2019	Alaska Department of Fish and Game / NOAA small-mesh trawl survey
Northern shrimp (*Pandalus eous*)	Chiniak Bay catch per unit effort, log-transformed	1977–2019	Alaska Department of Fish and Game / NOAA small-mesh trawl survey
Capelin (*Mallotus villosus*)	Pavlof Bay catch per unit effort, log-transformed	1972–2019	Alaska Department of Fish and Game / NOAA small-mesh trawl survey
Eulachon (*Thaleichthys pacificus*)	Pavlof Bay catch per unit effort, log-transformed	1972–2019	Alaska Department of Fish and Game / NOAA small-mesh trawl survey
Eulachon (*Thaleichthys pacificus*)	Chiniak Bay catch per unit effort, log-transformed	1977–2019	Alaska Department of Fish and Game / NOAA small-mesh trawl survey
Jellyfish	Pavlof Bay catch per unit effort, log-transformed	1972–2019	Alaska Department of Fish and Game / NOAA small-mesh trawl survey
Jellyfish	Chiniak Bay catch per unit effort, log-transformed	1977–2019	Alaska Department of Fish and Game / NOAA small-mesh trawl survey
Pacific herring (*Clupea pallasii*)	Mature Sitka Sound biomass	1979–2016	Alaska Department of Fish and Game assessment model
Pacific cod (*Gadus macrocephalus*)	Pavlof Bay catch per unit effort, log-transformed	1972–2019	Alaska Department of Fish and Game / NOAA small-mesh trawl survey
Pacific cod (*Gadus macrocephalus*)	Chiniak Bay catch per unit effort, log-transformed	1977–2019	Alaska Department of Fish and Game / NOAA small-mesh trawl survey
Coho salmon (*Oncorhynchus kisutch)*	Southeast Alaska commercial catch, lagged 1 year and log-transformed	1972–2018	Alaska Department of Fish and Game
Coho salmon (*Oncorhynchus kisutch)*	Prince William Sound commercial catch, lagged 1 year and log-transformed	1972–2018	Alaska Department of Fish and Game
Coho salmon (*Oncorhynchus kisutch)*	Kodiak commercial catch, lagged 1 year and log-transformed	1972–2018	Alaska Department of Fish and Game
Coho salmon (*Oncorhynchus kisutch)*	Cook Inlet commercial catch, lagged 1 year and log-transformed	1972–2018	Alaska Department of Fish and Game
Coho salmon (*Oncorhynchus kisutch)*	Chignik commercial catch, lagged 1 year and log-transformed	1972–2018	Alaska Department of Fish and Game
Coho salmon (*Oncorhynchus kisutch)*	South Alaska Peninsula commercial catch, lagged 1 year and log-transformed	1972–2018	Alaska Department of Fish and Game
Pink salmon (*Oncorhynchus gorbuscha*)	Southeast Alaska commercial catch, lagged 1 year and log-transformed	1972–2018	Alaska Department of Fish and Game
Pink salmon (*Oncorhynchus gorbuscha*)	Kodiak commercial catch, lagged 1 year and log-transformed	1972–2018	Alaska Department of Fish and Game
Pink salmon (*Oncorhynchus gorbuscha*)	Chignik commercial catch, lagged 1 year and log-transformed	1972–2018	Alaska Department of Fish and Game
Pink salmon (*Oncorhynchus gorbuscha*)	South Alaska Peninsula commercial catch, lagged 1 year and log-transformed	1972–2018	Alaska Department of Fish and Game
Lower-trophic level biology			
Spring bloom date	Surface chl-a	1998–2019	SeaWiFS, MODIS-Aqua
Spring bloom duration	Surface chl-a	1998–2019	SeaWiFS, MODIS-Aqua
Spring bloom amplitude	Surface chl-a	1998–2019	SeaWiFS, MODIS-Aqua
Pacific cod (*Gadus macrocephalus*)	Standardized spring ichthyoplankton density, fourth-root transformed	1982–2015	NOAA Ichthyoplankton Survey
Walleye pollock (*Gadus chalcogrammus*)	Standardized spring ichthyoplankton density, fourth-root transformed	1982–2015	NOAA Ichthyoplankton Survey
Rockfish (*Sebastes* spp.).	Standardized spring ichthyoplankton density, fourth-root transformed	1982–2015	NOAA Ichthyoplankton Survey
Ronquils (*Bathymaster* spp.)	Standardized spring ichthyoplankton density, fourth-root transformed	1982–2015	NOAA Ichthyoplankton Survey
Pacific sand lance (*Ammodytes personatus*)	Standardized spring ichthyoplankton density, fourth-root transformed	1982–2015	NOAA Ichthyoplankton Survey
Flathead sole (*Hippoglossoides elassodon*)	Standardized spring ichthyoplankton density, fourth-root transformed	1982–2015	NOAA Ichthyoplankton Survey
Northern rock sole (*Lepidopsetta polyxystra*)	Standardized spring ichthyoplankton density, fourth-root transformed	1982–2015	NOAA Ichthyoplankton Survey
Calanoid copepod biomass	May biomass, log transformed	1998–2018	UAF Seward Line
Calanoid copepod biomass	September biomass, log-transformed	1998–2018	UAF Seward Line
Euphausid biomass	May biomass, log transformed	1998–2018	UAF Seward Line
Euphausid biomass	September biomass, log-transformed	1998–2018	UAF Seward Line

(*continued on next page*)

Table 1 (*continued*)

Variable	Metric	Years	Source
Calanoid copepod size	Average size, May	1998–2018	UAF Seward Line
Calanoid copepod size	Average size, September	1998–2018	UAF Seward Line
Euphausid size	Average size, May	1998–2018	UAF Seward Line
Euphausid size	Average size, September	1998–2018	UAF Seward Line
Euphausid abundance	Density, log transformed	1997–2019	NOAA Icy Strait Survey
Pelagic amphipod abundance	Density, log transformed	1997–2019	NOAA Icy Strait Survey
Pelagic gastropod abundance	Density, log transformed	1997–2019	NOAA Icy Strait Survey
Large copepod abundance	Density, log transformed	1997–2019	NOAA Icy Strait Survey
Small copepod abundance	Density, log transformed	1997–2019	NOAA Icy Strait Survey
Copepod community size	Normalized anomaly	2000–2018	Marine Biological Association UK Continuous Plankton Recorder
Diatom abundance	Log-transformed, normalized anomaly	2000–2018	Marine Biological Association UK Continuous Plankton Recorder
Large copepod abundance	Log-transformed, normalized anomaly	2000–2018	Marine Biological Association UK Continuous Plankton Recorder
Mesozooplankton abundance	Log-transformed, normalized anomaly	2000–2018	Marine Biological Association UK Continuous Plankton Recorder
Small copepod abundance	Log-transformed, normalized anomaly	2000–2018	Marine Biological Association UK Continuous Plankton Recorder

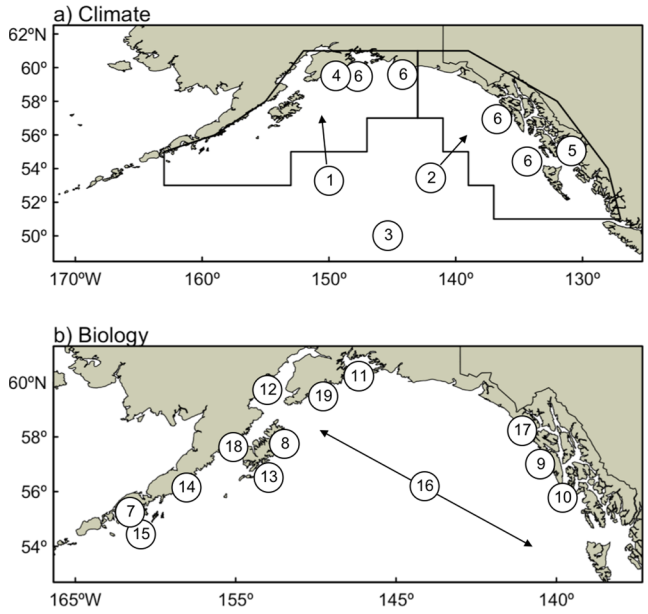

Fig. 1. Study site: approximate locations of a) climate time series, b) biology time series. 1 = western SST, 2 = eastern SST, 3 = Papa advection index, 4 = GAK1 site and northern end of SLP gradient, 5 = southern end of SLP gradient, 6 = upwelling stations, 7 = Pavlof Bay trawl survey, 8 = Chiniak Bay trawl survey, 9 = herring biomass, 10 = Southeast salmon catch, 11 = Prince William Sound salmon catch, 12 = Cook Inlet salmon catch, 13 = Kodiak salmon catch, 14 = Chignik salmon catch, 15 = South Peninsula salmon catch, 16 = Continuous Plankton Recorder, 17 = Icy Strait zooplankton, 18 = Shelikof ichthyoplankton, 19 = Seward Line zooplankton.

conventional DFA models in that it optionally allows for the deviations of the latent trends to be modeled with a Student-t, rather than Gaussian distribution. The Student-t distribution allows greater flexibility, particularly in modeling extreme events (Anderson et al., 2017). The Student-t distribution introduces a single scaling parameter υ; when υ is small the distribution of process variation includes a greater probability of extremes than the normal distribution, and when υ is large (~30) the year to year deviations are nearly identical to those drawn from a normal distribution. As implemented in Stan, we conducted estimation with 3 parallel chains, with a warm-up period of 2000 samples, followed by 2000 iterations. The potential scale reduction factor (Gelman and Rubin, 1992) and estimated Rhat were used to assess convergence (Rhat $<$ 1.05). Code to replicate these analyses is deployed as an R package on CRAN ('bayesdfa', Ward et al. 2019) and our public Github repository (https://github.com/fate-ewi/bayesdfa).

We used a model selection approach to evaluate the best-supported number of latent DFA trends from a candidate set of models invoking 1–3 trends. Each model was evaluated with two candidates for observation error structure (unique or shared observation error variances for individual time series). The best number of trends and best error structure were selected using the Bayesian Leave-One-Out Information Criterion (LOOIC; Vehtari et al., 2017). Model structures that failed convergence tests were removed from the analysis. We also rejected models that failed to load on any time series (using 90% or more of the posterior distribution as a threshold).

In the case of biology data, time series related to fisheries management (salmon catches, herring recruitment, small-mesh trawl survey catches, rockfish growth) were available going back to at least the early 1970 s, while lower trophic level time series (phytoplankton, zooplankton, and ichthyoplankton) were available only beginning in the 1980 s or 1990 s (Table 1). Attempts to fit DFA models to the full set of biology time series failed to converge and/or produced models with no loadings with posterior distributions that were 90% above or below zero. Accordingly, we fit separate DFA models to the two subsets of the biology data.

After identifying the best supported DFA model for the climate data and the two subsets of biology data described above, we conducted *post hoc* examination for evidence of state shifts in shared trends of variability (objective 2). We tested for the presence of alternative states by fitting a Hidden Markov Model (HMM) to the posterior trend estimates from each model. An HMM is similar to a DFA or other state-space model in that it partitions total variance into a process and observation error component, but unlike other approaches the HMM treats the latent process as discrete rather than continuous. As before, we used LOOIC to identify the data support for the greatest number of alternative states, using candidate sets of 1–5 states.

2.4. Changing community responses to SST variability

We conducted time-dependent regressions between the shared trend in long-term biology data and an environmental variable (winter SST) to test the hypothesis of non-stationary climate-community relationships (objective 3). This analysis evaluated the slope of the shared community trend on SST during three periods: the period of elevated Aleutian Low variance (from the start of our biology data set in 1972 through 1988; Litzow et al., 2019, 2018), the period of reduced Aleutian Low variance (1989–2013), and the 2014–2019 warming event. Time-dependent regression was executed in a Bayesian framework to

account for the uncertainty in latent community trends. The plankton time series, which were generally short and included few observations in the 1980 s, were judged to be insufficient to support this time-dependent analysis. Accordingly, we fit a single regression on winter SST for the shared trend from those data sets.

2.5. Changing relationships among time series

We follow the approach of Litzow et al. (2019) to test for changing relationships between individual time series and shared trends of variability identified by DFA models (objective 4). This analysis was conducted separately on the climate and long-term biology data sets; plankton time series were judged to be too short for evaluating non-stationary relationships in the current study. We calculated correlations, on 25-year rolling windows, between each time series and trends from the best DFA model for the entire data set. The 25-year window length was selected, based on earlier analysis (Litzow et al., 2019), as being short enough to resolve changing relationships but long enough to minimize the influence of stochastic variability. These correlations were conducted on the full DFA posteriors in a Bayesian framework to provide a probabilistic account of uncertainty. DFA models are interpreted in terms of stationary loadings that are assumed to be valid across the full time series under consideration (Ward et al., 2019; Zuur et al., 2003b). Therefore, correlations between population time series and DFA trends that change over time are evidence that such a time-independent interpretation is inappropriate. The 25-year length of durations was selected as a reasonable minimum length that might avoid spurious results based on stochastic noise in relationships. However, we recognize that this window length offers little power for detecting post-2014 changes in relationships. We therefore also compare loadings from separate DFA models to the climate and biology data from two periods: 15 years spanning the 1976/77 PDO shift (1972–1986) and the last 15 years of the data (2005–2019). Our aim here is not to examine the effects of nonstationary Aleutian Low variance as described in section *2.4*, but rather to determine if patterns of multivariate climate and biology change across the 2014–2019 warm anomaly are comparable to those associated with the 1970 s event.

3. Results

3.1. Comparison of observed and preindustrial SST (objective 1)

The 2014–2019 period includes the four warmest years since 1900 in the ERSSTv5 time series (Fig. 2). One year (2015) returned a FAR = 1 for each of the five models considered (Table 2), indicating that such an extreme anomaly was never matched in preindustrial simulations (Walsh et al., 2018b). Three other years (2014, 2016, 2019) produced FAR = 1 for four of the five models considered, and 2018 produced FAR = 1 for three models. Results for three-year running mean anomalies were uniformly strong, with FAR = 1 for all four models considered (Table 2), indicating that the duration and magnitude of recent anomalies would likely be impossible absent anthropogenic forcing.

The magnitude of temperature change associated with the 2014–2019 warming anomaly appears to be much greater than that associated with the 1976/77 PDO shift. Change in the three-year running mean of SST associated with the 1976/77 event (maximum range in anomalies around the shift event) was approximately 1.75 SD, while the 2014 event involved a ~ 3 SD change in SST anomalies (Fig. 2).

3.2. Ecosystem variability (objective 2) and changing community-SST relationships (objective 3)

The best DFA model for shared variability in Gulf of Alaska climate was a one-trend model with time series-specific observation error variances. The latent trend positively loaded all four SST time series, the SLP gradient, the Papa advection index, and upwelling at 54°N 134°W, and negatively loaded GAK1 salinity (Fig. 3a). The shared climate trend showed markedly elevated values during 2014–2019 (Fig. 3b).

Variability in the long-term biology time series was best described by a one-trend model with time series-specific observation error variances. This trend suggested coherence among salmon, herring, jellyfish and crustacean abundance time series, and opposite dynamics with capelin and shrimp abundance (Fig. 4a). The shared trend captured rapid community change following the 1970 s PDO shift, and did not show evidence of an abrupt shift associated with the 2014–2019 climate perturbation (Fig. 4b). The slope of this biology trend on winter SST showed a clear distinction between the eras of high Aleutian Low variance (1972–1988) and reduced Aleutian Low variance (1989–2013). In the high variance era, the SST effect was strongly positive, with 100% of the posterior distribution for the slope on SST being > 0 (slope in standardized units; Fig. 5). In the low variance era, the effect was not strongly different from zero, with 70% (30%) of the posterior distribution falling below (above) zero. While few years of post-2014 data are available, there is some suggestion of a strengthening effect of SST in these years, with 86% (14%) of the posterior distributions falling above (below) zero (Fig. 5).

The best model for lower-trophic level variability invoked a single latent trend with the same observation variance for all time series. This model indicated coherence among phytoplankton, zooplankton, and ichthyoplankton over a large area of the Gulf of Alaska (Fig. 6a). The trend showed low-frequency periods of positive and negative anomalies (Fig. 6b). This single trend showed a strong negative response to SST variability across the entire time series, with > 99% of the posterior distribution for slope falling below 0 (Fig. 6c).

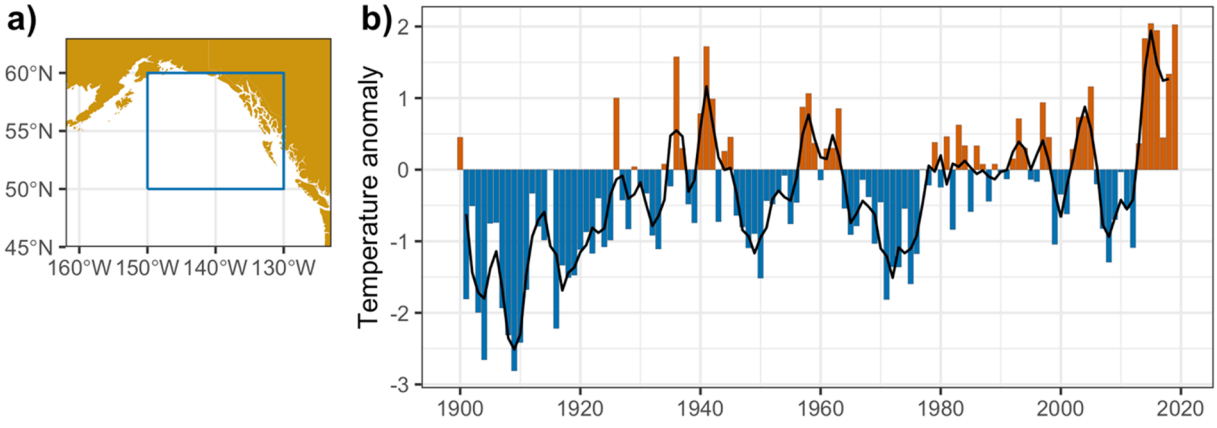

Fig. 2. Observed Gulf of Alaska SST anomalies for comparison with preindustrial simulations. a) Area in the Gulf of Alaska for which observations and simulations are compared. b) Time series of area-weighted annual anomalies from ERSSTv5. Black line plots three-year running mean anomalies.

Table 2
Fraction of attributable risk (FAR) for observed Gulf of Alaska sea surface temperature (SST) relative to simulated preindustrial values from five CMIP5 models.

Year(s)	Anomaly (SD)	CCSM4	GFDL.CM3	GISS.E2.R	IPSL.CM5A.LR	MRI.CGCM3
Annual anomalies						
2014	1.83	1	1	0.75	1	1
2015	2.04	1	1	1	1	1
2016	1.95	1	1	0.67	1	1
2017	0.45	0.87	0.6	0.2	1	0.4
2018	1.34	1	0.6	0.8	1	0.8
2019	2.03	1	1	0.5	1	1
Three-year means						
2014–2016	1.94	1	1	1	1	*
2017–2019	1.27	1	1	1	1	*

* Excluded from three-year running mean comparison.

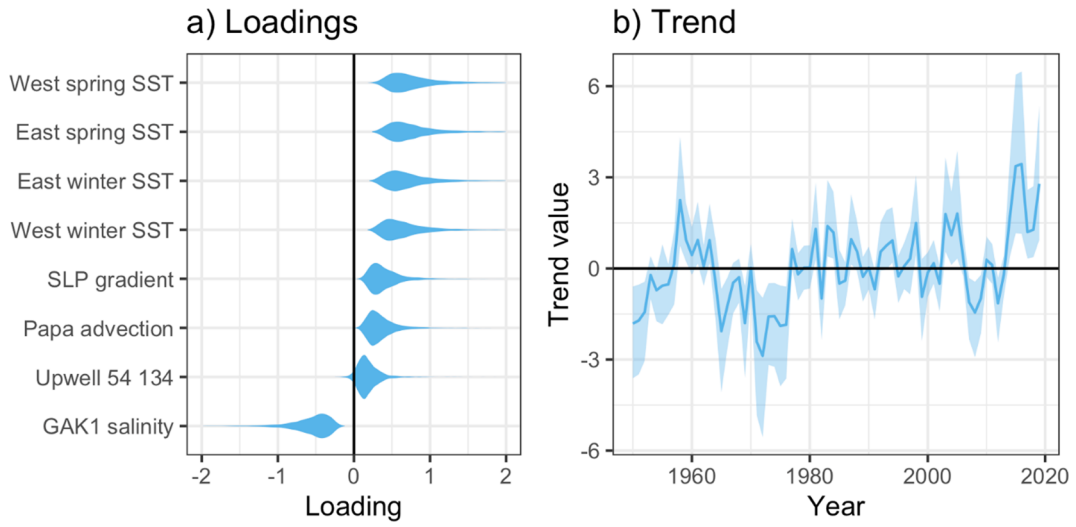

Fig. 3. Bayesian DFA estimates of shared variability in Gulf of Alaska climate variables, 1950–2019. a) Posterior distributions for loadings on individual time series, b) Shared trend time series with 95% credible interval.

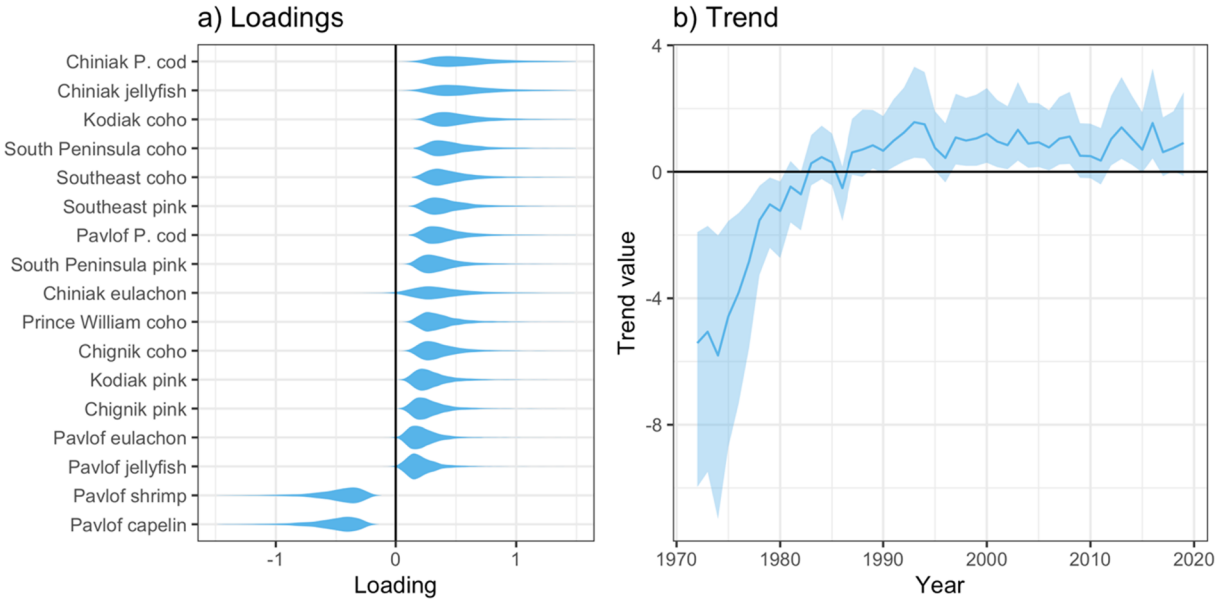

Fig. 4. Bayesian DFA estimates of shared variability among Gulf of Alaska population time series, 1972–2017. a) Posterior distributions for loadings on individual time series, b) Shared trend time series with 95% credible interval.

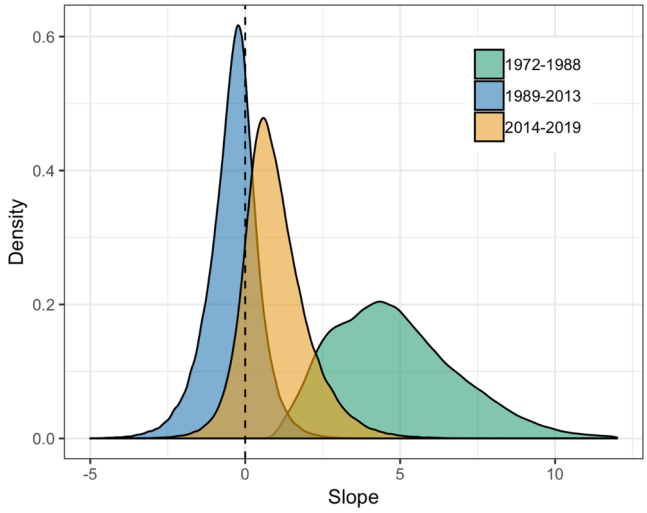

Fig. 5. Nonstationary community responses to climate variability: era-specific posteriors for the slope of the shared trend in long-term biology data on winter SST. Slope is in units of standard deviation (scaled anomaly).

Table 3
Results for Hidden Markov Model (HMM) evaluations for the evidence of state shifts in latent trends for different data sets. Entries are leave one out information criterion (LOOIC) values, with the best-supported model in each case indicated by bold.

Number of states	Climate data (1950–2019)	Salmon, herring, trawl survey data (1972–2019)	Plankton data (1981–2019)
1	241.18	154.46	67.01
2	**22.05**	**2.88**	**33.98**
3	50.11	7.56	59.43
4	74.94	13.55	79.34
5	92.73	18.61	95.55

3.3. Evidence for ecosystem state shifts (objective 2)

For most of the 2014–2019 period, median values for the latent trend in climate time series were beyond the range of previous observations (Fig. 3b). On the other hand, latent trends for the long-term biology and plankton data sets remained within the range of previous observations during 2014–2019 (Fig. 4b, 6b). After applying HMM

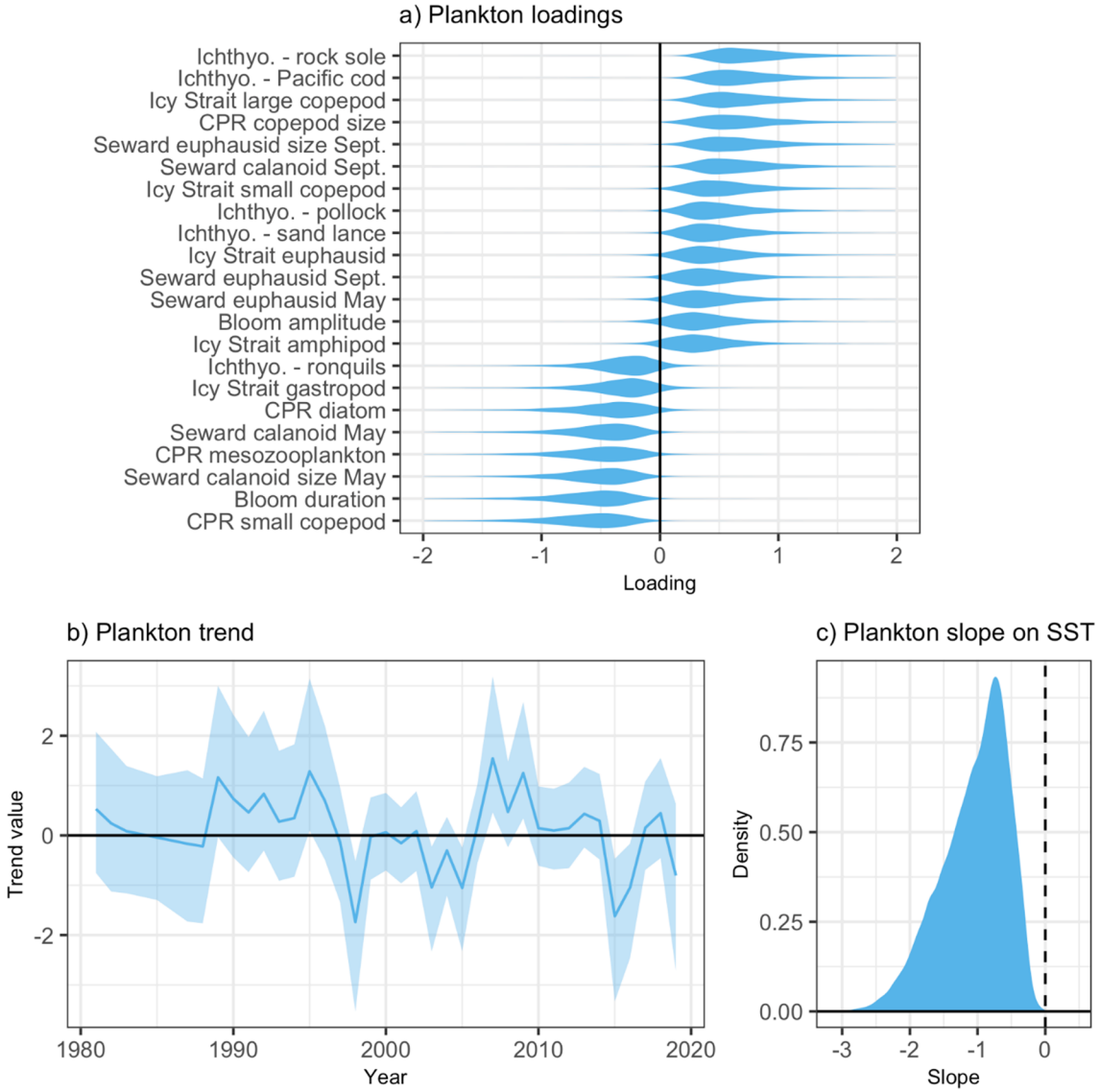

Fig. 6. DFA model fit to low trophic level time series (phytoplankton, ichthyoplankton and zooplankton). a) Posterior distributions for time series loadings, b) Shared trend and 95% credible interval, c) Posterior distribution for the slope of the shared trend on winter SST for the entire time series.

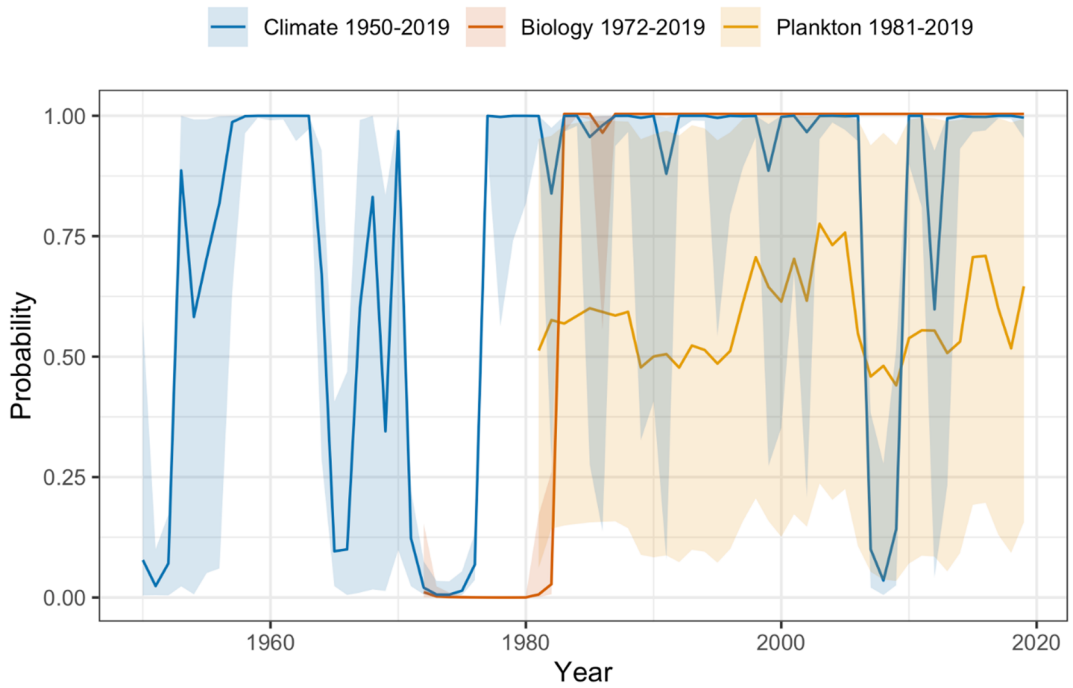

Fig. 7. State probability for latent trends in three Gulf of Alaska ecosystem data sets: Hidden Markov Model (HMM) results. The best model for all three data sets invoked two states, and the median probability of being in the state associated with warmer conditions is plotted for each, with 95% credible intervals. The probability of being in the state associated with colder conditions is the inverse of the plotted values.

models to trends from the three datasets to identify underlying hidden states, we found the strongest support for only two alternate states in each data set (Table 3). In each case, these alternate states were associated with relatively warmer and colder conditions, and none of HMM models supported the hypothesis of the emergence of novel alternate states during 2014–2019 (Fig. 7). We therefore conclude that our analysis does not find evidence of a shift to a novel mean state in shared trends of ecosystem variability during the 2014–2019 warm anomaly.

3.4. Nonstationary relationships among time series (objective 4)

Rolling correlations between individual climate time series values and the shared climate trend indicated that relationships among climate variables were nonstationary over the period that we consider (Fig. 8). Temperature time series showed periods of weakening correlations, centered roughly around the late 1980 s, followed by strengthening correlations later in the time series. Other time series showed more monotonic changes, consisting of either a general trend of weakening correlations (SLP gradient, Papa advection index, GAK1 salinity, and upwelling at 60°N 146°W) or strengthening correlations (the two southern upwelling stations). Rolling correlations between individual biology time series and the shared biology trend showed widespread evidence of nonstationary relationships (Fig. 9). Correlations for most time series weakened around the late 1980 s, and these correlations have generally remained weak for the remainder of the time series.

DFA models fit separately to data spanning the 1970 s PDO shift (1972–1986) and data for the recent anomaly (2005–2019) illustrate the changing nature of ecological variability in this system. Loadings for the four SST variables were similar for DFA models fit to climate data from the two periods. However, a number of other ecologically-important climate variables showed a tendency towards weaker loadings (posterior distributions shifted towards zero). This group included GAK1 salinity, upwelling at 60°N 146°W, the Papa advection index, and the SLP gradient (Fig. 10a). The model fit to 1972–1986 climate data clearly captured the 1970 s PDO shift (Fig. 10b), while the model fit to 2005–2019 data captured the unprecedented climate state that has pertained during 2014–2019 (Fig. 10c). The significance of the different loadings in the two eras informs interpretation of the two climate shifts illustrated in Fig. 10: the 1970 s event included stronger changes across all climate time series, while the 2014–2019 event has, by comparison, been more limited to change in temperature.

Finally, DFA models fit to biology data from the same two periods illustrate even greater changes in loadings (Fig. 11a), indicating that patterns of community change associated with the 1970 s event are not directly comparable with community responses to the 2014–2019 perturbation. Many biology time series show evidence of reversing signs of loadings in the later era (Pavlof and Chiniak shrimp, Southeast herring, Pavlof eulachon, Southeast coho and pink salmon, Pavlof Pacific cod). Some time series (Kodiak and South Peninsula pink salmon) show weaker loadings in 2005–2019 than in 1972–1986, similar to the weaker loadings in the second era seen for some climate time series. And still other time series show loadings that are similar between the two eras (Fig. 11a). The shared trend from the 1972–1986 model clearly captures the late 1970 s community shift (Fig. 11b). This ecological change was detected with a short (0–1 year) lag following the 1976/77 PDO shift, confirming the ability of our selected time series to provide a short-lag indication of ecological change following climate perturbations. To evaluate our ability to detect a community shift with limited data, we conducted a comparison HMM analysis for biology data limited to 1972–1982 (i.e., for data extending six years after the 1976/77 SST increase, corresponding to the six years of data available following the 2013/14 temperature increase). This analysis detected the 1976/77 community shift immediately (0–1 year lag), suggesting that data availability did not prevent the detection of an immediate community shift following the 2014 temperature increase (results not shown). The shared trend for the model fit to the 2005–2019 data shows elevated median values from 2016 onwards, suggesting some ecological response to the 2014–2019 warm anomaly, but the 95% credible interval for this trend includes 0 in every year (Fig. 11b). This result highlights the muted nature of recent ecological changes when compared to the 1972–1986 period, when strong patterns of change shared broadly across the community returned estimated trend values with 95% credible intervals below or above 0 for most years (Fig. 11b).

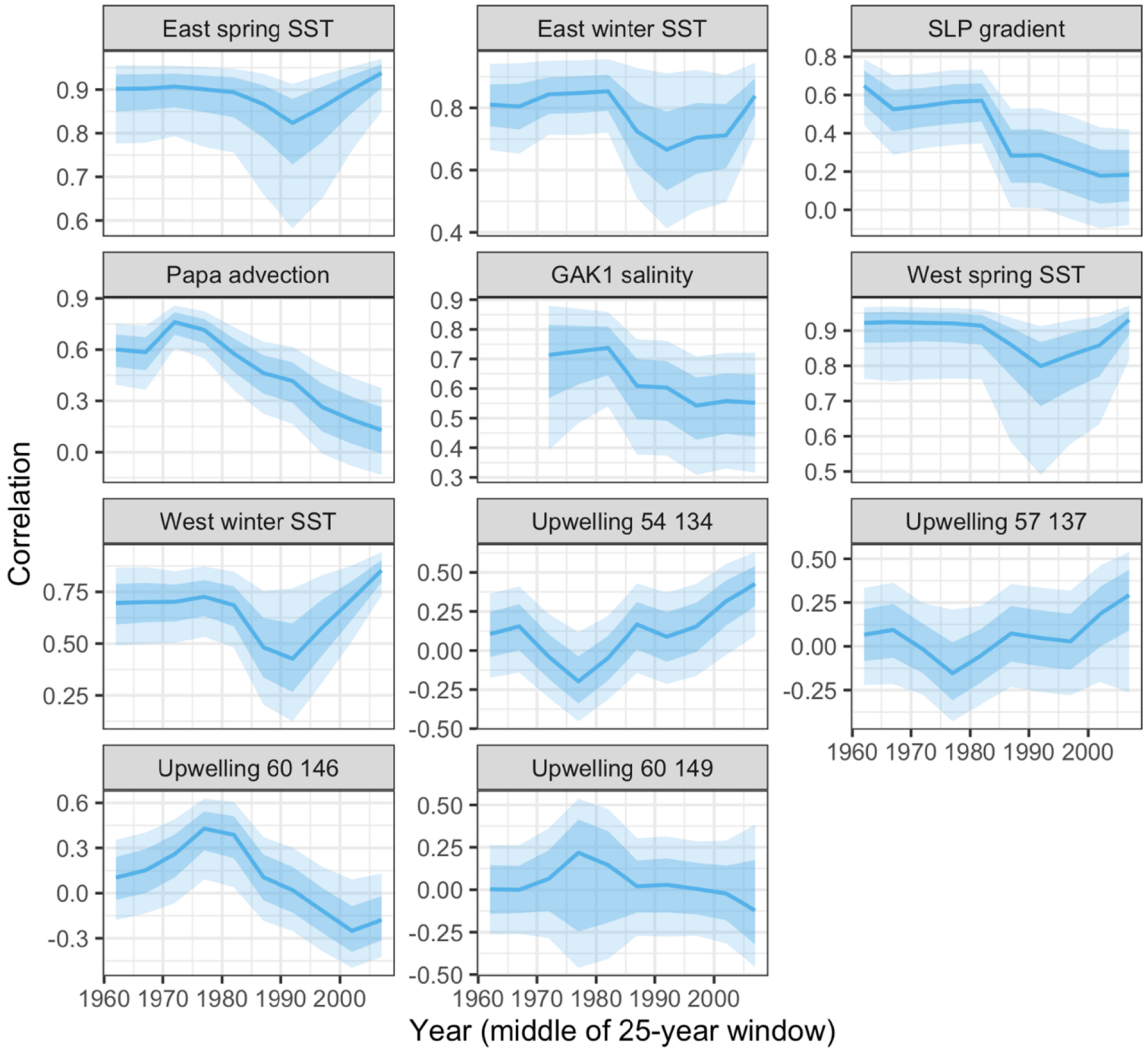

Fig 8. Nonstationary patterns of shared variability in Gulf of Alaska climate: Bayesian correlation between individual climate time series and the shared DFA trend for individual 25-year rolling correlations centered every 5 years between 1962 and 2007. Plots are median correlations with 50% and 80% quantiles of the posterior distribution. Note different scales on y-axis.

4. Discussion

4.1. Negative evidence for an ecosystem state shift

The persistence of extreme SST anomalies in the Gulf of Alaska during 2014–2019 is well outside the envelope of simulated pre-industrial conditions. Mean SST anomalies for both three-year windows considered (2014–2016 and 2017–2019) returned FAR values of 1 when compared with preindustrial simulations for every model considered, leading to the conclusion that the 2014–2019 climate perturbation would be impossible without anthropogenic forcing. This result implies departure from the envelope of natural climate variability, signaling an increased risk of ecological surprises involving novel climate and community configurations (Williams and Jackson, 2007). Of particular note in terms of potential ecosystem consequences of the 2014–2019 event is the comparison with the 1976/77 PDO shift, which was associated with an abrupt, widespread, and persistent state shift in the Gulf of Alaska ecosystem (Fig. 4b; Anderson and Piatt, 1999; Litzow and Mueter, 2014). Judged in terms of the magnitude of change in SST (~3 SD change vs ~ 1.75 SD change in 1976/77, Fig. 2) and the range of acute ecological responses noted in the Introduction, the 2014–2019 anomaly would seem capable of producing a wholesale community reorganization of a magnitude comparable to that seen following the 1976/77 event. However, none of our tests for alternative states in shared trends of climatic and biological variability showed evidence of a post-2014 alternative state (Fig. 7). This negative result for a shift in climate state may be partly explained by the paucity of post-2014 observations; continuation of recent values in the shared trend in climate variability would appear intuitively consistent with an alternative post-2014 state. However, red noise (autocorrelated random variability) creates shifts around the anthropogenic trend that are impossible to predict (Di Lorenzo and Ohman, 2013; Rudnick and Davis, 2003), so the persistence of 2014–2019 climate conditions over the short term future (i.e., < 10 years) cannot be robustly predicted. In addition, community responses to the 2014–2019 perturbation may occur with a time lag, in which case extended observations would be needed to detect change. However, the ability of biology time series selected for this study to provide a short-lag indication of ecological response to the 1976/77 event (Fig. 11b) argues against this consideration. We recognize that differences in pre-shift community states may also mediate differences in response to the 1976/77 and 2014–2019 climate perturbations. For instance, the low-diversity pre-1976/77 community state may have been inherently less stable than the higher-diversity community experiencing the 2014–2019 event (Frank et al., 2006). Rather than being an analogous ecological event to the 2014–2019 perturbation, the 1976/77 event is useful in terms of evaluating the

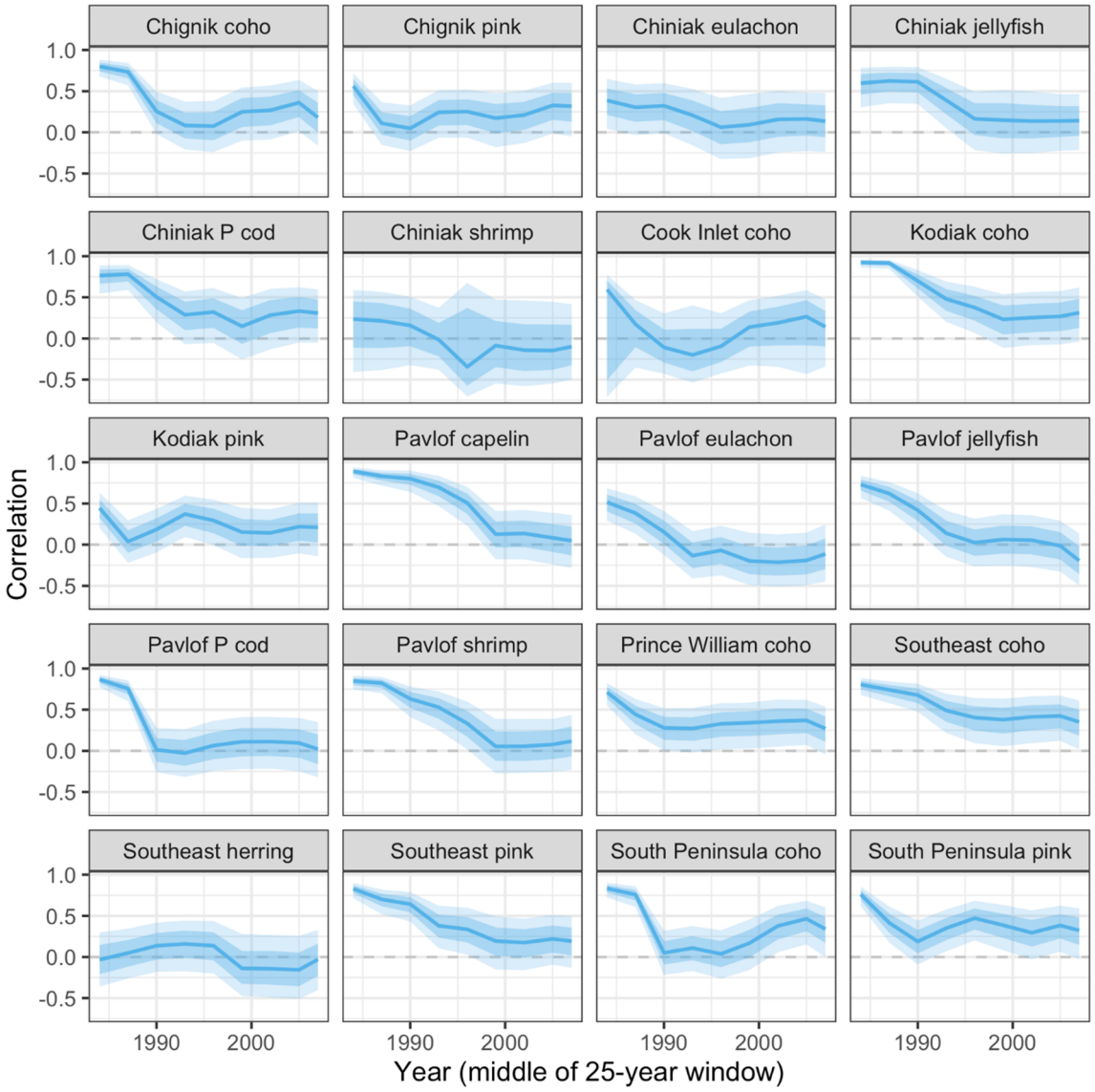

Fig 9. Nonstationary patterns of shared variability in the Gulf of Alaska community: Bayesian correlation between individual biology time series and the shared DFA trend for individual 25-year rolling correlations centered every 3 years between 1984 and 2007. Plots are median correlations with 50% and 80% quantiles of the posterior distribution.

ability of our data and methods to rapidly detect a community shift. We conclude that our results are consistent with resilience in the current community state, in spite of the many anecdotal reports of dramatic biological responses to heatwave conditions.

4.2. Changing community responses to temperature variability

A result that may suggest the potential for a community-level response to the current climate perturbation is the observation that statistical relationships between SST and the shared trend in long-term biology data may be reverting towards positive values after decades of a more neutral relationship (Fig. 5). While too few observations are yet available to provide firm inference concerning post-2014 SST-community relationships, this tentative result is consistent with observations that Aleutian Low variance is again increasing after the post-1988/89 period of low Aleutian Low variance (Litzow et al., 2020). Given past observations that periods of high (low) Aleutian Low variance appear to correspond with strong (weak) community responses to SST variability (Litzow et al., 2019, 2018; Puerta et al., 2019), these increases in Aleutian Low variability would suggest a reversion to strong community responses to SST variability, and the results in Fig. 5 appear consistent with this idea. However, a separate analysis suggests that salmon production took on a novel, negative correlation with SST and the PDO during 2014–2019 (Litzow et al., in press), which would seem to conflict with the possible reversion to a positive relationship demonstrated here. These conflicting results speak to the difficulty inherent in evaluating the effect of novel climate conditions with limited observations. In addition, loadings on several non-temperature climate time series during 2005–2019 remain weaker than loadings observed during 1972–1986 (Fig. 10a), suggesting that covariance between temperature and other climate variables remains weaker during the 2014–2019 climate anomaly than was the case with the 1970 s PDO shift, which would suggest an expectation of a weaker ecological response to the later event. While data limitations precluded the analysis of changing responses of lower trophic level taxa to temperature with the DFA modeling approach used in this study, Batten et al. (2018) found that positive temperature effects on diatom abundance and zooplankton abundance observed during 2000–2013 in the CPR data set were absent during the especially warm years of 2014–2015. These observations suggest the potential for further nonstationary responses to temperature variability, beyond those discussed above.

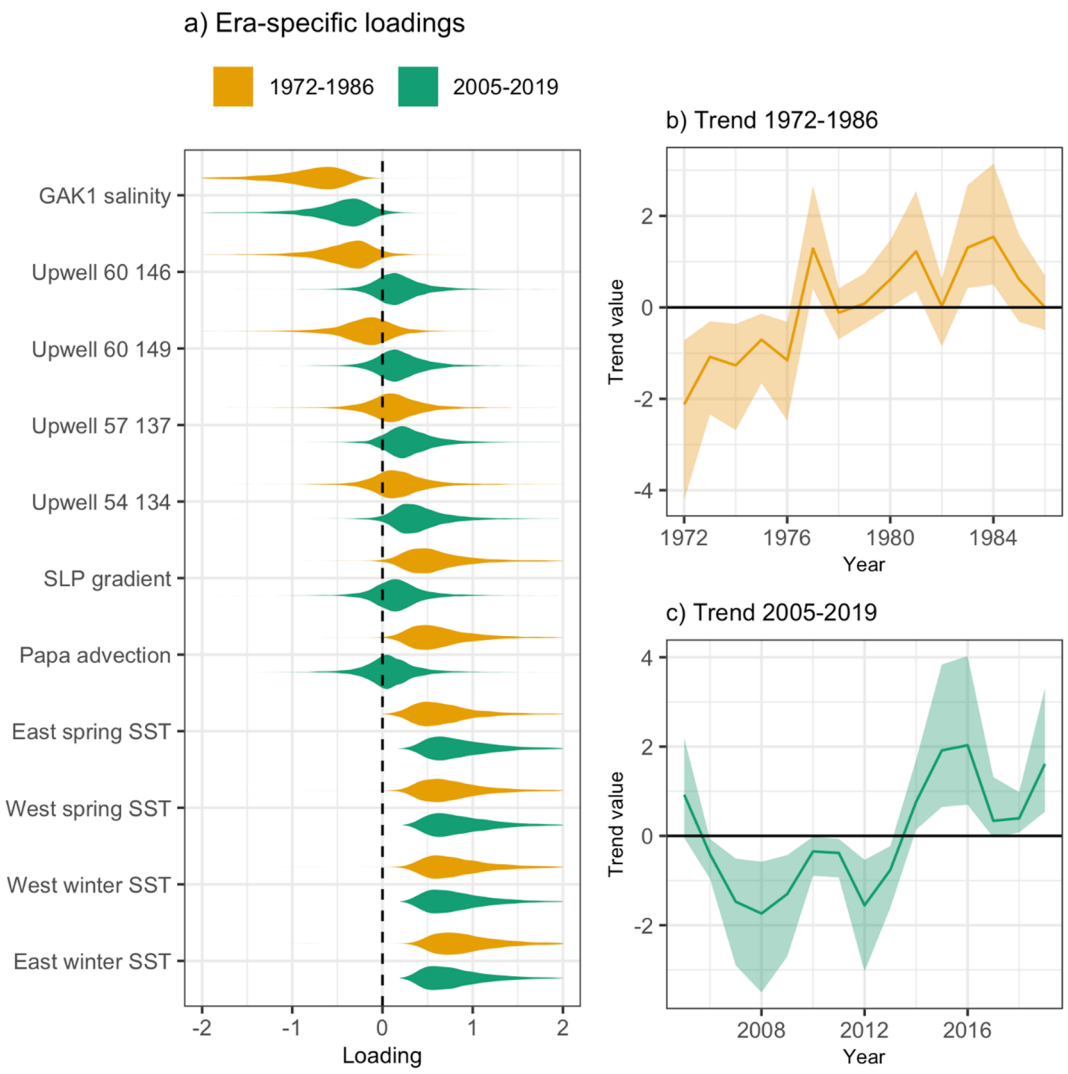

Fig. 10. Changing relationships among climate time series: results for DFA models fit separately to data from 1972–1986 and 2005–2019. a) Time series loadings for each era, b) Shared trend with 95% credible interval, 1972–1986, c) Shared trend with 95% credible interval, 2005–2019.

4.3. Lower trophic level responses to 2014–2019 warming

The DFA model fit to lower trophic level data is notable for identifying a latent trend that is broadly shared across multiple trophic levels and taxonomic groups (phytoplankton, zooplankton, and ichthyoplankton) over the spatial scale of a large marine ecosystem (Fig. 6a). The negative slope of this shared trend on winter SST (Fig. 6c) and low values in the shared trend during some anomalously warm years (2015, 2016, 2019; Fig. 6b) provide evidence of bottom-up climate effects on ecosystem productivity. The single shared trend produced by the DFA model provides only a first-order understanding of what are doubtless highly complex lower trophic level responses to the 2014–2019 warming event. One interpretation that may be useful for framing an initial understanding of these results is the observation that twice as many abundance, biomass, or size time series are predicted to show a negative response to warming (i.e., those with a positive DFA loading, $n = 14$) as are predicted to show a positive response (those with a negative DFA loading, $n = 7$; Fig. 6a). Results for several sets of individual time series merit discussion in this context. Loadings for ocean color time series indicate a longer spring bloom reaching a lower peak amplitude during warm years (98.7% chance of negative loadings for bloom duration, 91.8% chance of positive loadings for bloom amplitude). There was also some indication of earlier spring blooms with ocean warming (87.3% chance of positive loadings for bloom start date, not plotted). In the central Gulf of Alaska, warming and extreme SLP values associated with the onset of the 2014–2019 event are expected to increase upper water column stability, reduce mixing and lead to earlier nutrient depletion resulting in reduced primary productivity or a shift of the production into smaller cells (Bond et al., 2015; Peña et al., 2019). Dynamics on the continental shelf are likely more complex, in particular due to the role of terrigenous nutrient input (Batten et al., 2018; Coyle et al., 2019). While the interplay between bottom-up and top-down control in continental shelf ecosystems is complex (Frank et al., 2007; Litzow and Ciannelli, 2007), these changes in primary production have the potential to impact fisheries production in a warming Gulf of Alaska (Ware and Thomson, 2005). Given the complex nature of the changes suggested by these results (earlier, longer, lower-amplitude blooms), a more detailed analysis to consider higher-order effects such as the potential for temporal mismatches with secondary consumers would be warranted to better elucidate the potential ecosystem consequences of these changes.

Zooplankton loadings on the shared trend also suggest complicated responses to warming, though several themes emerge from the results. Positive loadings on copepod time series for the CPR, Icy Strait, and Seward Line data sets indicate a reduction in copepod abundance and size with ocean warming. These effects include opposite loadings for Seward Line calanoid copepod abundance in May (negative loading) and September (positive loading), indicating a switch to increased

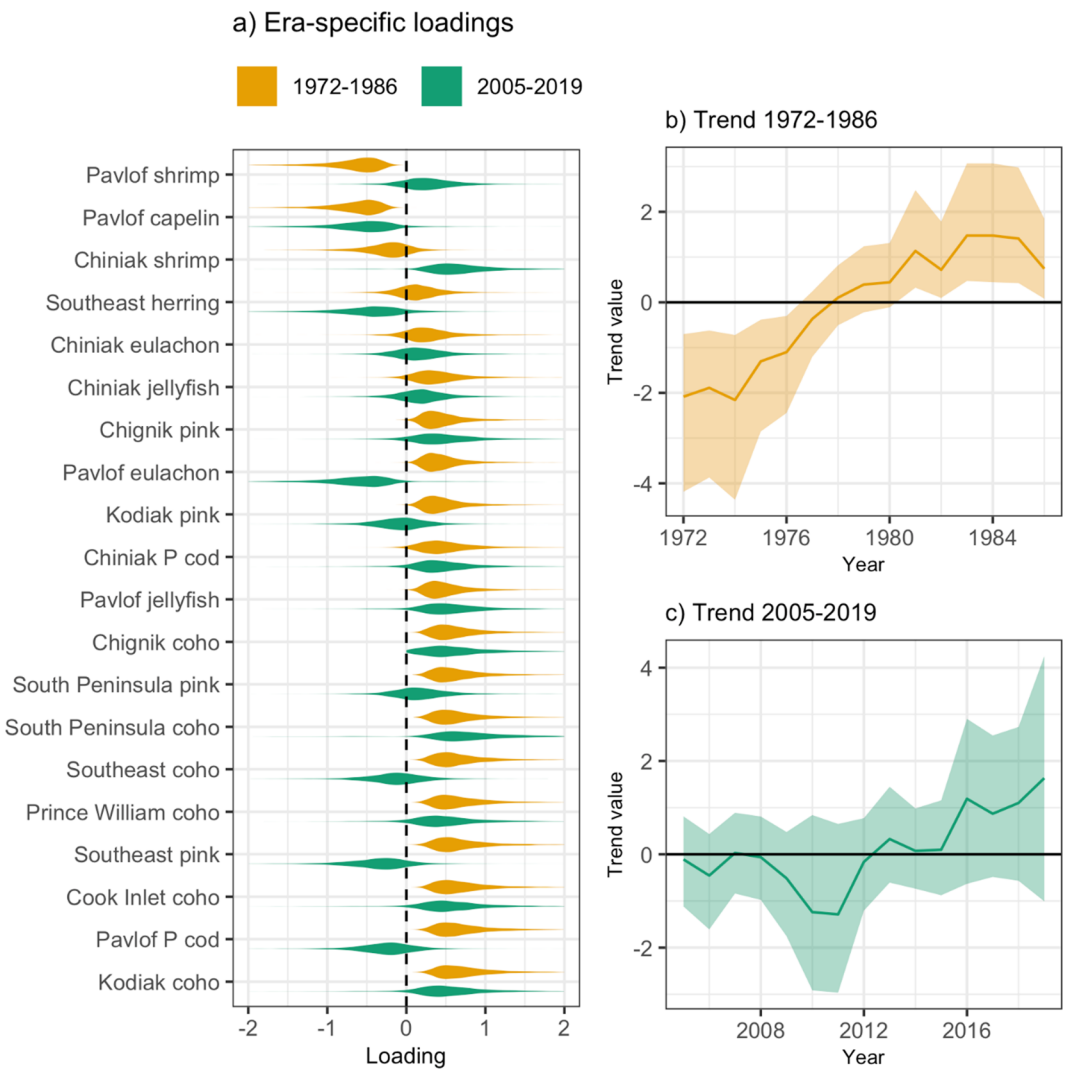

Fig. 11. Changing relationships among biology time series: results for DFA models fit separately to data from 1972–1986 and 2005–2019. a) Time series loadings for each era, b) Shared trend with 95% credible interval, 1972–1986, c) Shared trend with 95% credible interval, 2005–2019.

(decreased) abundance early (late) in the season as a response to warming, which may indicate coherence with the earlier bloom timing noted above. This interpretation is supported by modeling work suggesting bottom-up control of springtime calanoid biomass in the system (Coyle et al., 2019). Ichthyoplankton loadings on the shared trend were almost entirely positive, indicating a decline in abundance for a variety of commercially and ecologically important taxa during the warming event. These taxa include walleye pollock, which support the largest groundfish fishery in the Gulf of Alaska, rockfish, another important commercial group, and Pacific cod, which supported an important fishery prior to their recent stock collapse. Also notable in this context is the positive loading on Pacific sand lance, indicating reduced larval abundance for this species during the 2014–2019 warm period, which is consistent with observations of strongly negative growth and energy density anomalies for this species during the warming event (von Biela et al., 2019). These generally negative relationships between ichthyoplankton abundance and winter temperature may reflect the negative effects of increased metabolic rates that result in the early depletion of larval lipid reserves (Doyle et al., 2019). Alternately, the peak timing of ichthyoplankton abundance in the spring is believed to reflect synchrony with the spring bloom (Doyle et al., 2019), so the earlier timing of the spring bloom might indicate a phenological mismatch with larval energetic demand. These are only preliminary speculations concerning the mechanisms underlying the patterns we show here, and the mechanistic links between rapid warming and community responses are likely to be highly complex.

4.4. Novel climate and community combinations

A central assumption for most dimensional reduction techniques is that relationships among different variables are stationary over the time period under consideration (i.e., they are described by a probability density that does not change over time; Kolmogorov, 1991). In the case of DFA, this assumption is expressed through the requirement that model residuals should be independent and identically distributed (Zuur et al., 2003b). A central idea from paleoecology is that over long time scales, the assumption of stationary relationships required for these techniques is not met; over time, climates and communities take on new combinations that cannot be summarized with fixed statistical definitions (Maguire et al., 2015; Williams and Jackson, 2007). An analogous situation apparently occurred in the Gulf of Alaska after the 1988/89 decline in Aleutian Low variance. The switch from strong covariance to weak covariance among climatic and biological time series resulted in significant autocorrelation in regression and DFA model residuals, indicating time-dependent errors in inference (Litzow et al., 2019, 2018). While these findings suggest that common statistical approaches assuming stationary relationships are inappropriate for this system, there are few commonly-used approaches for dimensional

reduction that allow time-dependent relationships to be modeled. Accordingly, we took a hybrid approach in this study: we used a novel implementation of an increasingly popular dimensional reduction technique assuming stationary relationships (Bayesian DFA) to identify the strongest patterns of shared variability within the data sets, but also used rolling correlations and model fitting to subsets of data to illustrate temporal changes in relationships that cannot be captured by DFA. The problem of changing ecological relationships will only grow in importance as anthropogenic climate change accelerates (Williams and Jackson, 2007; Wolkovich et al., 2014), and improved statistical approaches will be needed to support robust understanding of changing ecosystem function and identity.

The rolling window analysis of correlations between individual time series and the shared trends of climatic and biological variability (Figs. 8, 9) are consistent with the hypothesis of nonstationary relationships among ecosystem variables in the Gulf of Alaska. The changes in correlations for a number of climate time series are centered around the late 1980 s (Fig. 8), consistent with the timing of the decline in Aleutian Low variance as a proposed deterministic cause of nonstationary relationships in the physical environment. There was no indication of sudden changes in correlations for climate variables at the end of the time series that would be consistent with a sudden change in relationships since 2014, though the 25-year windows used in this analysis would have limited sensitivity to changes over the last six years of the time series. The increase in strength of correlations between the four SST time series and the shared climate trend in the second half of the time series (Fig. 8) is consistent with the idea of a reversion towards strong multivariate collinear relationships for SST in this system. However, loadings for a number of non-temperature climate time series remain weaker in the model fit to 2005–2019 data than to 1972–1986 data (Fig. 10a), suggesting that patterns of shared covariance among climate time series remain relatively weak during the 2014–2019 warming event when compared with the 1976/77 PDO shift. None of the climate variables show evidence of loadings with different signs between the two periods (Fig. 10a), so we conclude there is little evidence for novel climate combinations as an outcome of the 2005–2019 warming event.

On the other hand, DFA models fit to biology data for the two periods return a number of time series with opposite sign loadings, indicating strong differences in the nature of community variability over time. These time-dependent loadings have important implications for the ways in which ecological variability is measured over time, as they imply that common dimensional reduction techniques that assume stationary loadings over time are likely inadequate for resolving patterns of community variability over the historical record in this ecosystem. This result also loops back to the evidence that 2014–2019 SST anomalies were outside the envelope of natural variability (Table 2). As the climate of this ecosystem has exceeded the bounds of historical variability, historical understanding of climate-biology relationships and patterns of community variability is increasingly likely to fail (Williams and Jackson, 2007). While the absence of evidence for ecosystem state changes during the 2014–2019 indicates ecological resilience during this event, the unprecedented nature of this climate perturbation sounds a cautionary note about the potential for outsized ecosystem consequences with continued warming.

Declaration of Competing Interest

The authors declare that they have no known competing financial interests or personal relationships that could have appeared to influence the work reported in this paper.

Acknowledgements

Funding for this project came from NOAA's Fisheries and the Environment (FATE) program (project 16-01). We thank John Walsh for generously sharing previously published CMIP5 outputs, and Nick Bond, Mike Jacox, and John Walsh for helpful input concerning comparison of observed SST with preindustrial simulations. We also thank Kally Spalinger for sharing small-mesh trawl survey data, and the many scientists from the Alaska Department of Fish and Game and National Marine Fisheries Service for conducting this survey for so many decades. We also thank the many scientists who have contributed to the maintenance of the other long-term data sets used in this study; meaningful understanding of the Gulf of Alaska ecosystem over decadal time scales would be impossible without their efforts.

References

Anderson, S.C., Branch, T.A., Cooper, A.B., Dulvy, N.K., 2017. Black-swan events in animal populations. Proc. Natl. Acad. Sci. 114, 3252–3257. https://doi.org/10.1073/pnas.1611525114.

Anderson, P.J., Piatt, J.F., 1999. Community reorganization in the Gulf of Alaska following ocean climate regime shift. Mar. Ecol. Prog. Ser. 189, 117–123.

Auth, T.D., Daly, E.A., Brodeur, R.D., Fisher, J.L., 2018. Phenological and distributional shifts in ichthyoplankton associated with recent warming in the northeast Pacific Ocean. Glob. Chang. Biol. 24, 259–272. https://doi.org/10.1111/gcb.13872.

Batten, S.D., Raitsos, D.E., Danielson, S., Hopcroft, R., Coyle, K., McQuatters-Gollop, A., 2018. Interannual variability in lower trophic levels on the Alaskan Shelf. Deep. Res. part II-Topical Stud. Oceanogr. 147, 58–68. https://doi.org/10.1016/j.dsr2.2017.04.023.

Bond, N.A., Cronin, M.F., Freeland, H., Mantua, N., 2015. Causes and impacts of the 2014 warm anomaly in the NE Pacific. Geophys. Res. Lett. 42, 3414–3420. https://doi.org/10.1002/2015GL063306.

Brodeur, R.D., Auth, T.D., Phillips, A.J., 2019. Major shifts in pelagic micronekton and macrozooplankton community structure in an upwelling ecosystem related to an unprecedented marine heatwave. Front. Mar. Sci. 6. https://doi.org/10.3389/fmars.2019.00212.

Carpenter, B., Gelman, A., Hoffman, M.D., Lee, D., Goodrich, B., Betancourt, M., Brubaker, M.A., Guo, J., Li, P., Riddell, A., 2017. Stan: A Probabilistic Programming Language. J. Stat. Softw. 76, 1–29. https://doi.org/10.18637/jss.v076.i01.

Cavole, L.-C.M., Demko, A.M., Diner, R.E., Giddings, A., Koester, I., Pagniello, C.M.L.S., Paulsen, M.-L., Ramirez-Valdez, A., Schwenck, S.M., Yen, N.K., Zill, M.E., Franks, P.J.S., 2016. Biological Impacts of the 2013–2015 Warm-Water Anomaly in the Northeast Pacific. OCEANOGRAPHY 29, 273–285. https://doi.org/10.5670/oceanog.2016.32.

Coyle, K.O., Hermann, A.J., Hopcroft, R.R., 2019. Modeled spatial-temporal distribution of productivity, chlorophyll, iron and nitrate on the northern Gulf of Alaska shelf relative to field observations. Deep. Res. part II-Topical Stud. Oceanogr. 165, 163–191. https://doi.org/10.1016/j.dsr2.2019.05.006.

Di Lorenzo, E., Ohman, M.D., 2013. A double-integration hypothesis to explain ocean ecosystem response to climate forcing. Proc. Natl. Acad. Sci. 110, 2496–2499.

Doyle, M.J., Strom, S.L., Coyle, K.O., Hermann, A.J., Ladd, C., Matarese, A.C., Shotwell, S.K., Hoperoft, R.R., 2019. Early life history phenology among Gulf of Alaska fish species: Strategies, synchronies, and sensitivities. Deep. Res. PART II-TOPICAL Stud. Oceanogr. 165, 41–73. https://doi.org/10.1016/j.dsr2.2019.06.005.

Duffy-Anderson, J.T., Stabeno, P., Andrews III, A.G., Cieciel, K., Deary, A., Farley, E., Fugate, C., Harpold, C., Heintz, R., Kimmel, D., Kuletz, K., Lamb, J., Paquin, M., Porter, S., Rogers, L., Spear, A., Yasumiishi, E., 2019. Responses of the northern Bering Sea and southeastern Bering Sea pelagic ecosystems following record-breaking low winter sea ice. Geophys. Res. Lett. 46, 9833–9842. https://doi.org/10.1029/2019GL083396.

Frank, K.T., Petrie, B., Shackell, N.L., 2007. The ups and downs of trophic control in continental shelf ecosystems. Trends Ecol. Evol. 22, 236–242. https://doi.org/10.1016/j.tree.2007.03.002.

Frank, K.T., Petrie, B., Shackell, N.L., Choi, J.S., 2006. Reconciling differences in trophic control in mid-latitude marine ecosystems. Ecol. Lett. 9, 1096–1105. https://doi.org/10.1111/j.1461-0248.2006.00961.x.

Gelman, A., Rubin, D.B., 1992. Inference from iterative simulation using multiple sequences. Stat. Sci. 7, 457–472.

Gomez-Ocampo, E., Gaxiola-Castro, G., Burazo, R., Beier, E., 2018. Effects of the 2013–2016 warm anomalies on the California Current phytoplankton. Deep. Res. part II-Topical Stud. Oceanogr. 151, 64–76. https://doi.org/10.1016/j.dsr2.2017.01.005.

Hare, S.R., Mantua, N.J., 2000. Empirical evidence for North Pacific regime shifts in 1977 and 1989. Prog. Oceanogr. 47, 103–145. https://doi.org/10.1016/s0079-6611(00)00033-1.

Henson, S.A., Beaulieu, C., Ilyina, T., John, J.G., Long, M., Seferian, R., Tjiputra, J., Sarmiento, J.L., 2017. Rapid emergence of climate change in environmental drivers of marine ecosystems. Nat. Commun. 8, 14682. https://doi.org/10.1038/ncomms14682.

Holmes, E.E., Ward, E.J., Scheuerell, M.D., 2018. Analysis of multivariate time-series using the MARSS package. Seattle, USA.

Huang, B., Thorne, P.W., Banzon, V.F., Boyer, T., Chepurin, G., Lawrimore, J.H., Menne, M.J., Smith, T.M., Vose, R.S., Zhang, H.-M., 2017. Extended reconstructed sea surface temperature, version 5 (ERSSTv5): Upgrades, validations, and intercomparisons. J. Clim. 30, 8179–8205. https://doi.org/10.1175/JCLI-D-16-0836.1.

Hunt, G.L., Stabeno, P.J., Strom, S., Napp, J.M., 2008. Patterns of spatial and temporal variation in the marine ecosystem of the southeastern Bering Sea, with special reference to the Pribilof Domain. Deep. Res. Part II-Topical Stud. Oceanogr. 55, 1919–1944. https://doi.org/10.1016/j.dsr2.2008.04.032.

Jacox, M.G., Alexander, M.A., Mantua, N.J., Scott, J.D., Hervieux, G., Webb, R.S., Werner, F.E., 2018. Forcing of multiyear extreme ocean temperatures that impacted California Current living marine resources in 2016. Bull. Am. Meteorol. Soc. 99, S27–S33. https://doi.org/10.1175/BAMS-D-17-0119.1.

Kolmogorov, A.N., 1991. Selected Works of A. N. Kolmogorov, Volume I: Mathematics and Mechanics. Springer Netherlands, Dordrecht, NL.

Leising, A.W., Schroeder, I.D., Bograd, S.J., Abell, J., Durazo, R., Gaxiola-Castro, G., Bjorkstedt, E.P., Field, J., Sakuma, K., Robertson, R.R., Goericke, R., Peterson, W.T., Brodeur, R., Barcelo, C., Auth, T.D., Daly, E.A., Suryan, R.M., Gladics, A.J., Porquez, J.M., McClatchie, S., Weber, E.D., Watson, W., Santora, J.A., Sydeman, W.J., Melin, S.R., Chavez, F.P., Golightly, R.T., Schneider, S.R., Fisher, J., Morgan, C., Bradley, R., Warybok, P., 2015. State of the California Current 2014–15: Impacts of the Warm-Water "Blob". Calif. Coop. Ocean. Fish. Investig. Reports 56, 31–68.

Litzow, M.A., Ciannelli, L., 2007. Oscillating trophic control induces community reorganization in a marine ecosystem. Ecol. Lett. 10, 1124–1134. https://doi.org/10.1111/j.1461-0248.2007.01111.x.

Litzow, M.A., Ciannelli, L., Puerta, P., Wettstein, J.J., Rykaczewski, R.R., Opiekun, M., 2019. Nonstationary environmental and community relationships in the North Pacific Ocean. Ecology 100, ecy.2760. https://doi.org/10.1002/ecy.2760.

Litzow, M.A., Ciannelli, L., Puerta, P., Wettstein, J.J., Rykaczewski, R.R., Opiekun, M., 2018. Non-stationary climate–salmon relationships in the Gulf of Alaska. Proc. R. Soc. B Biol. Sci. 285, 20181855. https://doi.org/10.1098/rspb.2018.1855.

Litzow, M.A., Hunsicker, M.E., Bond, N.A., Burke, B.J., Cunningham, C.J., Gosselin, J.L., Norton, E.L., Ward, E.J., Zador, S.G., 2020. The changing physical and ecological meanings of North Pacific Ocean climate indices. Proc. Natl. Acad. Sci. U. S. A. 117, 7665–7671. https://doi.org/10.1073/pnas.1921266117.

Litzow, M.A., Malick, M.J., Bond, N.A., Cunningham, C., Gosselin, J.L., Ward, E.J., in press. Quantifying a novel climate through changes in PDO-climate and PDO-salmon relationships. Geophys. Res. Lett. submitted.

Litzow, M.A., Mueter, F.J., 2014. Assessing the ecological importance of climate regime shifts: an approach from the North Pacific Ocean. Prog. Oceanogr. 120, 110–119. https://doi.org/10.1016/j.pocean.2013.08.003.

Litzow, M.A., Mueter, F.J., Hobday, A.J., 2014. Reassessing regime shifts in the North Pacific: incremental climate change and commercial fishing are necessary for explaining decadal-scale biological variability. Glob. Chang. Biol. 20, 38–50. https://doi.org/10.1111/gcb.12373.

Litzow, M.A., Urban, D., 2009. Fishing through (and up) Alaskan food webs. Can. J. Fish. Aquat. Sci. 66, 201–211. https://doi.org/10.1139/f08-207.

Maguire, K.C., Nieto-Lugilde, D., Fitzpatrick, M.C., Williams, J.W., Blois, J.L., 2015. Modeling species and community responses to past, present, and future episodes of climatic and ecological change. Annu. Rev. Ecol. Evol. Syst. 46 (46), 343–368. https://doi.org/10.1146/annurev-ecolsys-112414-054441.

Mantua, N.J., Hare, S.R., Zhang, Y., Wallace, J.M., Francis, R.C., 1997. A Pacific interdecadal climate oscillation with impacts on salmon production. Bull. Am. Meteorol. Soc. 78, 1069–1079. https://doi.org/10.1175/1520-0477(1997)078<1069:apicow>2.0.co;2.

Marshall, K.N., Duffy-Anderson, J.T., Ward, E.J., Anderson, S.C., Hunsicker, M.E., Williams, B.C., 2019. Long-term trends in ichthyoplankton assemblage structure, biodiversity, and synchrony in the Gulf of Alaska and their relationships to climate. Prog. Oceanogr. 170, 134–145. https://doi.org/10.1016/j.pocean.2018.11.002.

McCabe, R.M., Hickey, B.M., Kudela, R.M., Lefebvre, K.A., Adams, N.G., Bill, B.D., Gulland, F.M.D., Thomson, R.E., Cochlan, W.P., Trainer, V.L., 2016. An unprecedented coastwide toxic algal bloom linked to anomalous ocean conditions. Geophys. Res. Lett. 43. https://doi.org/10.1002/2016GL070023.

Morgan, C.A., Beckman, B.R., Weitkamp, L.A., Fresh, K.L., 2019. Recent Ecosystem Disturbance in the Northern California Current. Fisheries 44, 465–474. https://doi.org/10.1002/fsh.10273.

Newman, M., Alexander, M.A., Ault, T.R., Cobb, K.M., Deser, C., Di Lorenzo, E., Mantua, N.J., Miller, A.J., Minobe, S., Nakamura, H., Schneider, N., Vimont, D.J., Phillips, A.S., Scott, J.D., Smith, C.A., 2016. The Pacific Decadal Oscillation, revisited. J. Clim. 29, 4399–4427. https://doi.org/10.1175/JCLI-D-15-0508.1.

Peña, M.A., Nemcek, N., Robert, M., 2019. Phytoplankton responses to the 2014–2016 warming anomaly in the northeast subarctic Pacific Ocean. Limnol. Oceanogr. 64, 515–525. https://doi.org/10.1002/lno.11056.

Peterson, W.T., Fisher, J.L., Strub, P.T., Du, X., Risien, C., Peterson, J., Shaw, C.T., 2017. The pelagic ecosystem in the Northern California Current off Oregon during the 2014–2016 warm anomalies within the context of the past 20 years. J. Geophys. Res. 122, 7267–7290. https://doi.org/10.1002/2017JC012952.

Piatt, J., Parrish, J., Renner, H.M., Schoen, S.K., Jones, T., Kuletz, K.J., Arimitsu, M.L., Bodenstein, B., Garcia-Reyes, M., Duerr, R., Corcoran, R., Kaler, R., McChesney, G., Golightly, R., Coletti, H., Suryan, R.M., Burgess, H., Lindsey, J., Lindquist, K., Warzybok, P., Jahnke, J., Roletto, J., Sydeman, W.J., 2020. Extreme mortality and reproductive failure of common murres resulting from the northeast Pacific marine heatwave of 2014–2016. PLoS One 15, e0226087. https://doi.org/10.1371/journal.pone.0226087.

Puerta, P., Ciannelli, L., Rykaczewski, R., Opiekun, M., Litzow, M.A., 2019. Do Gulf of Alaska fish and crustacean populations show synchronous non-stationary responses to climate? Prog. Oceanogr. 175, 161–170. https://doi.org/10.1016/j.pocean.2019.04.002.

R Core Team, 2018. R: A language and environment for statistical computing. R Foundation for Statistical Computing, Vienna, Austria.

Roggatz, C.C., Fletcher, N., Benoit, D.M., Algar, A.C., Doroff, A., Wright, B., Wollenberg Valero, K.C., Hardege, J.D., 2019. Saxitoxin and tetrodotoxin bioavailability increases in future oceans. Nat. Clim. Chang. Doi: 10.1038/s41558-019-0589-3.

Rudnick, D.L., Davis, R.E., 2003. Red noise and regime shifts. Deep. Res. Part I-Oceanographic Res. Pap. 50, 691–699. https://doi.org/10.1016/s0967-0637(03)00053-0.

Stabeno, P.J., Bond, N.A., Hermann, A.J., Kachel, N.B., Mordy, C.W., Overland, J.E., 2004. Meteorology and oceanography of the Northern Gulf of Alaska. Cont. Shelf Res. 24, 859–897. https://doi.org/10.1016/j.csr.2004.02.007.

Stan Development Team, 2018. RStan: The R interface to Stan.

Stevenson, D.E., Lauth, R.R., 2019. Bottom trawl surveys in the northern Bering Sea indicate recent shifts in the distribution of marine species. Polar Biol. 42, 407–421. https://doi.org/10.1007/s00300-018-2431-1.

Stott, P.A., Stone, D.A., Allen, M.R., 2004. Human contribution to the European heatwave of 2003. Nature 432, 610–614. https://doi.org/10.1038/nature03089.

Trenberth, K.E., Hurrell, J.W., 1994. Decadal atmosphere-ocean variations in the Pacific. Clim. Dyn. 9, 303–319. https://doi.org/10.1007/bf00204745.

Vehtari, A., Gelman, A., Gabry, J., 2017. Practical Bayesian model evaluation using leave-one-out cross-validation and WAIC. Stat. Comput. 27, 1413–1432. https://doi.org/10.1007/s11222-016-9696-4.

von Biela, V.R., Arimitsu, M.L., Piatt, J.F., Heflin, B., Schoen, S.K., Trowbridge, J.L., Clawson, C.M., 2019. Extreme reduction in nutritional value of a key forage fish during the Pacific marine heatwave of 2014–2016. Mar. Ecol. Prog. Ser. 613, 171–182. https://doi.org/10.3354/meps12891.

Walsh, J.E., Bhatt, U.S., Littell, J.S., Leonawicz, M., Lindgren, M., Kurkowski, T.A., Bieniek, P.A., Thoman, R., Gray, S., Rupp, T.S., 2018a. Downscaling of climate model output for Alaskan stakeholders. Environ. Model. Softw. 110, 38–51. https://doi.org/10.1016/j.envsoft.2018.03.021.

Walsh, J.E., Thoman, R.L., Bhatt, U.S., Bieniek, P.A., Brettschneider, B., Brubaker, M., Danielson, S., Lader, R., Fetterer, F., Holderied, K., Iken, K., Mahoney, A., McCammon, M., Partain, J., 2018b. The high latitude heat wave of 2016 and its impacts on Alaska. Bull. Am. Meteorol. Soc. 99, S39–S43. https://doi.org/10.1175/BAMS-D-17-0105.1.

Ward, E.J., Anderson, S.C., Damaino, L.C., Hunsicker, M.E., Litzow, M.A., 2019. Modeling regimes with extremes: the bayesdfa package for identifying and forecasting common trends and anomalies in multivariate time series data. R J. 11, 46–55. https://doi.org/10.32614/RJ-2019-007.

Ware, D.M., Thomson, R.E., 2005. Bottom-up ecosystem trophic dynamics determine fish production in the northeast. Pacific. Science 308 (80), 1280–1284. https://doi.org/10.1126/science.1109049.

Weingartner, T.J., Danielson, S.L., Royer, T.C., 2005. Freshwater variability and predictability in the Alaska Coastal Current. Deep. Res. Part II-Topical Stud. Oceanogr. 52, 169–191. https://doi.org/10.1016/j.dsr2.2004.09.030.

Williams, J.W., Jackson, S.T., 2007. Novel climates, no-analog communities, and ecological surprises. Front. Ecol. Environ. 5, 475–482.

Wolkovich, E.M., Cook, B.I., McLauchlan, K.K., Davies, T.J., 2014. Temporal ecology in the Anthropocene. Ecol. Lett. 17, 1365–1379. https://doi.org/10.1111/ele.12353.

Zuur, A.F., Fryer, R.J., Jolliffe, I.T., Dekker, R., Beukema, J.J., 2003a. Estimating common trends in multivariate time series using dynamic factor analysis. Environmetrics 14, 665–685. https://doi.org/10.1002/env.611.

Zuur, A.F., Tuck, I.D., Bailey, N., 2003b. Dynamic factor analysis to estimate common trends in fisheries time series. Can. J. Fish. Aquat. Sci. 60, 542–552.